J Mater Sci (2007) 42:9434–9439
DOI 10.1007/s10853-007-1842-0

Effects of duty ratio at high frequency on growth mechanism of micro-plasma oxidation ceramic coatings on Ti alloy

Zhongping Yao · Yanli Jiang · Zhaohua Jiang · Fuping Wang

Received: 11 December 2006 / Accepted: 9 May 2007 / Published online: 26 July 2007
© Springer Science+Business Media, LLC 2007

Abstract The aim of this work is to study the effects of duty ratio on the growth mechanism of the ceramic coatings on Ti–6Al–4V alloy prepared by pulsed single-polar MPO at 2,000 Hz in $NaAlO_2$ solution. The phase composition of the coatings was studied by X-ray diffraction, and the morphology and the element distribution in the coating were examined through scanning electron microscopy and energy dispersive spectroscopy. The thickness of the coatings was measured by eddy current coating thickness gauge. The corrosion resistance of the coated samples was examined by linear sweep voltammetry technique in 3.5% NaCl solution. Duty ratio influenced the composition and structure of the coatings. Many residual discharging channels on the coating surface showed that the spark discharge at 2,000 Hz was mainly attributable to the breakdown of the oxide film, which was suitable for the elements both from the electrolyte and from the substrate to join MPO process, and therefore, the coating was mainly composed of Al_2TiO_5. Because of the increase of the congregation and the adsorption of Al from the electrolyte with increasing duty ratio, the redundant Al on the electrode surface led to the formation of γ-Al_2O_3. And Al and Ti in the coating existed in the form of the reverse gradient distribution. Meantime, ceramic coatings improved the corrosion resistance of Ti alloy, and the coating surface morphology and thickness determined the coated samples prepared at $D = 20\%$ had the best corrosion resistance among the coated samples.

Introduction

There is much recent interest about micro-plasma oxidation (MPO) because of the fine properties of the ceramic coatings prepared by this technique and many application prospects in many fields such as aviation, naval vessels, biomedicine, chemical industry, and so on [1–4]. Indeed, some applications have been reported on the MPO of Al alloys and Mg alloys. Up to now, the similar or relevant applications on the MPO of Ti alloys are reported nowhere except in Russia [5–8].

At present, much research is focused on the preparation and the properties of MPO coatings. And there are also a few instances of research on the growth mechanism of MPO ceramic coatings on Al alloys and Mg alloys, but such work on the growth mechanism of ceramic coatings on Ti alloys are rarely studied by the researchers [9–12]. Among the technique parameters for the widely used pulsed (bi-polar and single-polar) power source for MPO technique, the most often investigated are the electrolyte, the reaction time and the current density because of their importance. However, the frequency and the duty ratio, which are investigated a little, also play important roles in the coating growth and the coating properties [13–17]. Such research on the frequency and the duty ratio would be very useful and urgent to reveal the growth mechanism of the ceramic coatings on Ti alloys and quicken the possible application of such coatings in some fields. In our previous

Z. Yao
School of Materials Science and Engineering, Harbin Institute of Technology, Harbin 150001, PR China

Z. Yao (✉) · Y. Jiang · Z. Jiang · F. Wang
Department of Applied Chemistry, Harbin Institute of Technology, Harbin 150001, PR China
e-mail: yaozhongping@hit.edu.cn

Y. Jiang
Department of Life Science and Chemistry, Harbin University, Harbin 150086, PR China

work, we studied the effects of duty ratio at low frequency on growth mechanism of micro-plasma oxidation ceramic coatings on Ti alloy, and found the changes of duty ratio at low frequency led to the changes of the mode of the spark discharge, which further influenced the structure, the morphology and the corrosion resistance of the ceramic coatings for the pulsed single-polar micro-plasma oxidation [18]. In this paper, we used pulsed single-polar MPO power source to prepare ceramic coatings of different duty ratios under the condition of high frequency, and investigated the effects of duty ratio at high frequency on the growth mechanism of micro-plasma oxidation ceramic coatings. Meantime, the corrosion resistance of the coated samples was also discussed.

Experimental details

Preparation of the coatings

Disc samples of Ti–6Al–4V (mass%: 89.3 Ti, 6.26 Al, 4.01 V, 0.30 Fe, 0.10 C, 0.03 N) with a diameter of 16 mm and thickness of 6 mm were polished with abrasive paper. A home-made pulsed single-polar power source with a power of 5 kW was used for MPO of the disc samples in a water-cooled electrolyser made of stainless steel, which also serves as the counter electrode. The reaction temperature was controlled to below 30 °C by adjusting the cooling water flow. The MPO process equipment used is similar to the one presented by Matthews' group in Ref. [1]. The output mode of the anode pulse is seen in Fig. 1. D is the duty ratio of the anode pulse process and T is a working period. The electric parameters of the power source and

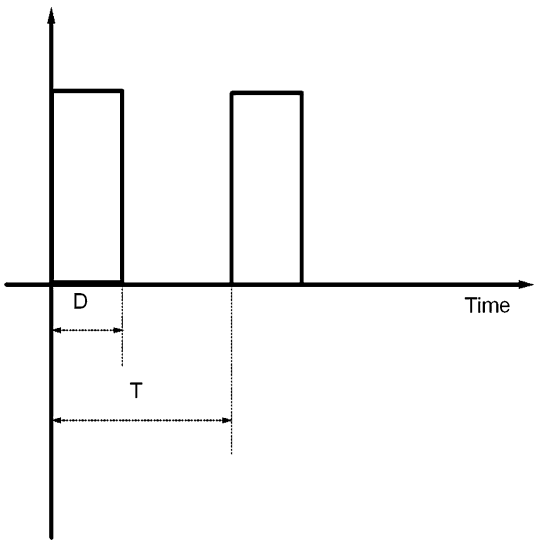

Fig. 1 The output mode of anode pulse for pulsed single-polar MPO power source D—duty ratio of anode pulse, T—a working period

Table 1 The electric parameters of the power source and reaction time during MPO process

No.	Frequency (Hz)	Current density (A/dm^2)	Duty ratio		Reaction time (min)
			D (%)	D_1 (ms)	
1	2000	20	10	0.05	60
2	2000	20	20	0.1	30
3	2000	20	30	0.15	20
4	2000	20	45	0.225	14

MPO reaction time was shown in Table 1. D_1 is the actual working time of the anode process within a period. The concentration of Na_2AlO_2 used in the experiment was 8 g/L and that of Na_3PO_4 was 1 g/L. After the treatment, the coated samples was rinsed with water and dried in air. Three samples were made under each condition to ensure the reliability of the experiments.

Phase composition and structure of the coatings

The morphology of the prepared coatings was studied with scanning electron microscopy (SEM; Hitachi S-570). The elemental distribution was investigated by energy dispersive spectroscopy (EDS; US PN5502). The phase composition of the coatings was examined with X-ray diffraction (XRD), using a Cu Kα source. The sample thickness was measured, using an eddy current-based thickness gauge (CTG-10, Time Company, China) with a minimum resolution of 1 μm. The average thickness of each sample was obtained from 10 measurements at different positions.

Corrosion resistance

In a three-electrode cell (Pt plate was used as counter electrode, a calomel electrode auxiliary reference electrode, and the coated sample as the working electrode), the corrosion resistance of the coated samples was evaluated from the linear sweep voltammetry technique in 3.5 wt% NaCl solution at room temperature through a CHI604c electrochemical analyzer (Shanghai, China). The scanning rate was 0.1 mV s^{-1}, with a scanning range from –30 mV to +30 mV of open circuit potential.

Results

Thickness of the coating

The thickness of the coatings changed with the electric parameters. It is known that the coating thickness was increased with the increasing current density or decreasing the working frequency [13, 15]. However, the duty ratio

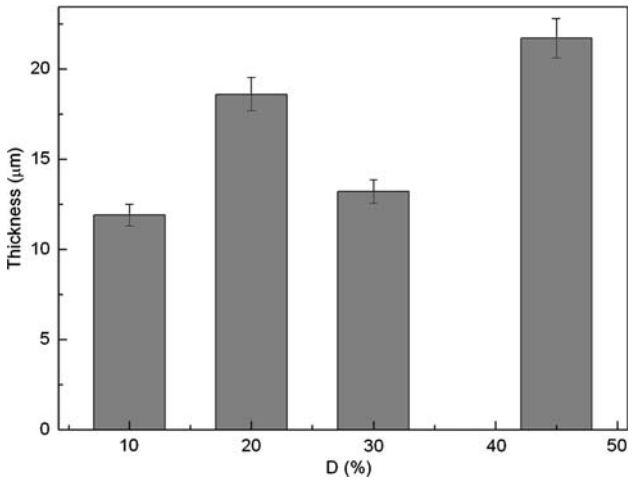

Fig. 2 Thickness of the coatings prepared under different duty ratios

(D) influenced the coating thickness differently with the results shown in Fig. 2. The coating thickness was increased with the increase of D in general. However, there was an exception: the thickness of the coatings prepared at $D = 20\%$ was larger than that at $D = 30\%$.

Surface SEM analyses of the coatings

Figure 3 is the surface SEM of the coatings with different duty ratios at 2,000 Hz. There are many residual discharging channels distributing evenly on the coating surface. And the diameters of the discharging channels are quite different: the bigger ones are 5–7 μm or so while the numerous smaller ones are less than 1 μm. Besides, the residual discharging channels were approximately a few microns deep, and pointed to all different directions. Increasing D, the mean diameters of the discharging channels was enlarged whereas the amount of them was lessoned correspondingly.

Section SEM and elemental distributions of the coatings

Figure 4 is the section image of the coating prepared at $D = 20\%$ and the results of EDS analysis in different positions of the coating are shown in Table 2. In the substrate near the interface, Ti and Al were lessened a little, and V was increased comparatively. This means that Ti and Al were both joined the MPO process. From the interface

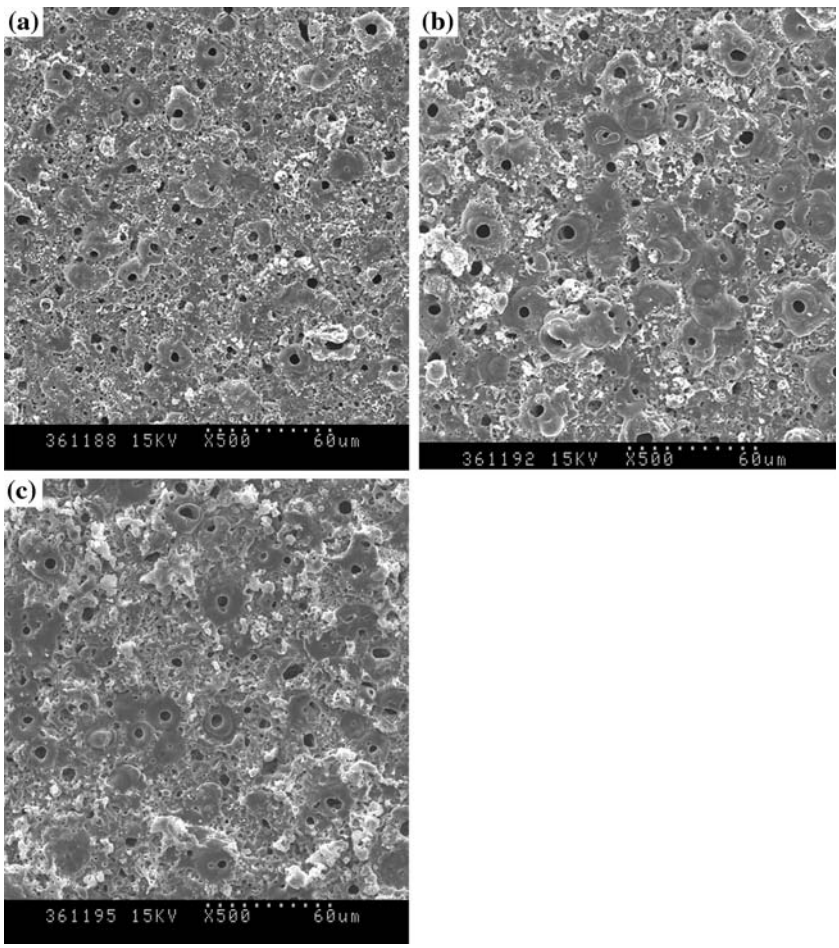

Fig. 3 Surface SEM of the coatings prepared under different duty ratios (**a**) $D = 10\%$, (**b**) $D = 20\%$, (**c**) $D = 30\%$

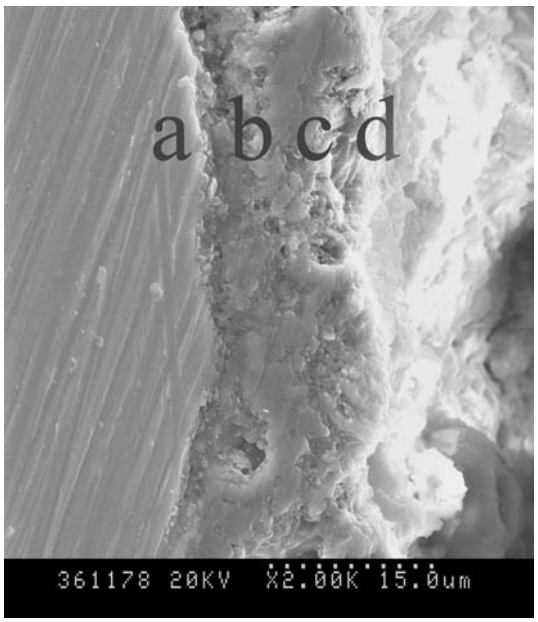

Fig. 4 The section image of the coatings prepared under D = 20%

Table 2 Relative content (mass%) of the main elements in the coating by EDS. a: Substrate; b: Inner coating; c: Middle coating; d: Outer coating

	(mass %)			
	Substrate	Inner coating	Middle coating	Outer coating
Al	5.4	18.8	21.3	35.0
Ti	88.9	77.1	75.1	60.8
V	5.7	3.9	3.6	4.2

to the coating surface, the content of Ti was decreased step by step while the content of Al was increased gradually. Meantime, V also came into the coating and may exist in the form of amorphous state because no crystallized substances containing V were detected by XRD analysis in 3.4. Clearly, Ti and V in the coating are from the substrate while Al in the coating is mainly from the electrolyte since the Al in the substrate is only 6.26% or so and cannot afford such a large amount for the coating growth.

XRD analysis of the coatings

Figure 5 is the XRD patterns of the ceramic coatings prepared at different duty ratios. The coatings are mainly composed of Al_2TiO_5; meantime there also exist a little γ-Al_2O_3, which was increased with increasing D. The diffraction peak corresponding to Ti substrate appeared because that coating was comparatively thin. Interestingly, the intensity of Al_2TiO_5 in the coating prepared at D = 20% is stronger than that at D = 10% and at D = 30%,

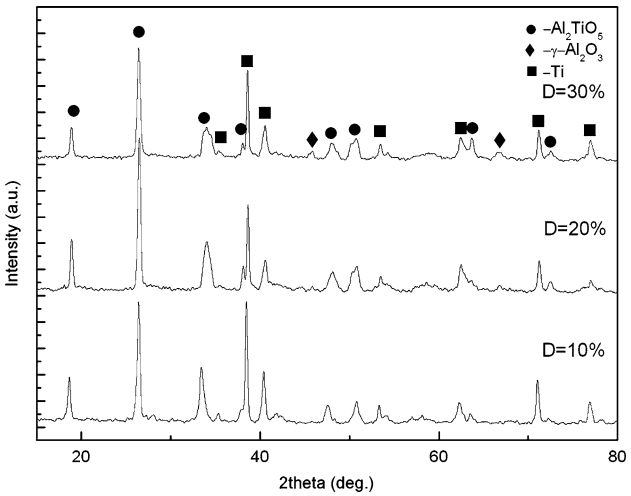

Fig. 5 XRD patterns of the coatings prepared under different duty ratios

which illustrates the content of Al_2TiO_5 in the coating prepared at D = 20% is more than other two conditions.

Corrosion resistance of the coated samples

The linear sweep voltammetry curves are shown in Fig. 6. And the corrosion potential and the polarization resistance (R_p) are presented in Table 3. Compared with the substrate, the corrosion resistance of the coated samples is better than that of the substrate, whether considering the corrosion potential or the polarization resistance. The corrosion potential of the coated samples increased with increasing D. However, R_p of the coated samples first increased with the increasing D, and reached the maximum when D = 20% and then decreased with increasing D. Generally, R_p can better reflect the corrosion resistance of the coated

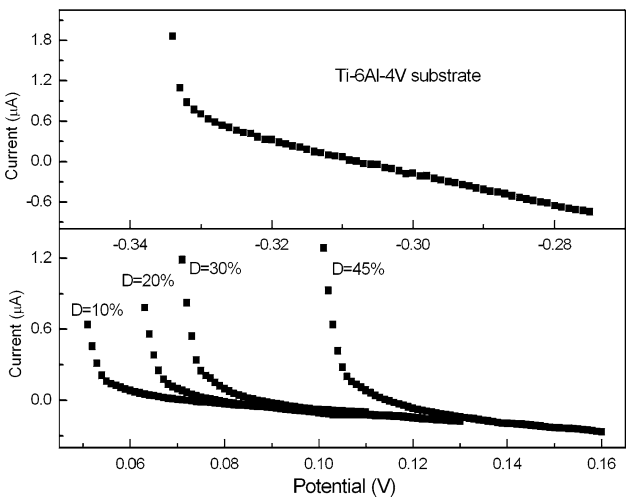

Fig. 6 Linear sweep voltammetry curves of the coated samples and the substrate in 3.5% NaCl solution

Table 3 Corrosion potential and polarization resistance (R_p) of the coated samples and the substrate

	Ti–6Al–4V	D = 10%	D = 20%	D = 30%	D = 45%
Corrosion potential (V)	–0.2961	0.0798	0.0860	0.1014	0.1260
R_p (Ω)	4.24×10^4	4.31×10^5	4.47×10^5	3.21×10^5	2.74×10^5

samples. Therefore, the corrosion resistance of the coated samples prepared at D = 20% was best.

Discussion on growth mechanism

According to Fig. 1, one working period of the power source includes an anode process and a dead time. The actual working time of the power source through the whole MPO process equals $D \times$ Reaction time. So, in order to study the effects of the duty ratio on the coatings under the fixed current density and frequency, it is important to adjust the reaction time to make sure that the actual working time through the whole MPO process is the same.

The ceramic coating is formed during the anode pulse process, and the power source was not at work and the electrode was cooled during the dead time. The spark discharge occurs when the working voltage reaches the breakdown voltage during anode pulse process. Because many residual discharging channels exist on the coating surface, it can be well estimated that the spark discharge at 2,000 Hz should be mainly attributable to the breakdown of the oxide film. In this way, the discharging channels are suitable not only for the entering of the congregated and adsorbed substances (like Al) from the electrolyte, but the transportation of the soluble substrate Ti as well, which means that both the electrolyte and the substrate joined MPO process on the electrode interface. During the dead time, the electrode interface was quickly cooled, and the melted substances in and near the discharge channels formed the coating accompanying the crystallizations, the complexion, the crystal transformation and the other processes, which led to the formation of a large amount of Al_2TiO_5. The formation of a little γ-Al_2O_3 in the coating with the increasing D is due to the increase of the D_1 of the anode pulse process. The congregation and the absorption of Al from the electrolyte on the electrode surface was increased with the increasing D_1, which provides redundant Al for the formation of Al_2O_3. And the formation of γ-Al_2O_3 in priority is because the nucleation free energy of γ-Al_2O_3 is lower than that of α-Al_2O_3 [17]. Therefore, γ-Al_2O_3 can be formed when $D \geq 20\%$, or in other words, when the D_1 is more than 0.1 ms in the experimental conditions.

Also, the average thickness of the coating is related to the absorption layer of Al from the electrolyte and the solution speed of Ti. On the one hand, the increase of D_1 is helpful for more Al from the electrolyte to form the Al_2O_3 in the coating, and more soluble Ti to form Al_2TiO_5, both of which are helpful for the increase of the coating thickness. On the other hand, the resistance of the absorption layer was also increased with increasing D_1, which would take up more working current (or voltage) and consequently reduce the solution speed of the substrate Ti. And the coating thickness is also one important factor, which increased the transportation resistance of the soluble Ti coming into the coating. Therefore, the formation speed of the Al_2TiO_5 was lessened, which would be liable to reduce the coating thickness. The two opposite effects competed with each other, which results into the abnormality of the thickness of the coating prepared at D = 20%. When $D \leq 20\%$, the former effect is stronger than the latter, which means that more Al_2O_3 and Al_2TiO_5 were formed in the coating to increase the coating thickness; When $D \geq 20\%$, the latter effect is stronger than the former, which means that Al_2TiO_5 was reduced to a certain extent, and the coating thickness was decreased consequently, although the content of Al_2O_3 was increased a little. This can be further proved by the forgoing analysis of coating composition in 3.4. If D was increased further, the increase of the content of Al_2O_3 would become the main factor for the increase of the coating thickness.

The increase of D_1 also extends the time of spark discharging, which is consistent with the phenomena observed in the experiments. The spark or the micro arc twinkled slowly with the increase of D_1. The discharging sparks got larger and less, and in this way the residual discharging channels on the surface of the prepared coatings became larger in size and decreased in number.

The corrosion resistance of the coated samples is mainly related to the thickness, the surface states and the composition of the coatings as well. Because all the coatings in the experiments are similar in the composition, therefore the surface morphology and thickness become important factors of the corrosion resistance for the coated samples. Based on the foregoing SEM analyses, there seems to be a conflict between the number and the size of the residual discharging channels on the coating surface. The coated samples prepared at D = 20% has the best corrosion resistance due to the results from the above conflict and the thickness factor somewhat.

Conclusions

The ceramic coatings were prepared on Ti–6Al–4V by pulsed single-polar micro-plasma oxidation at 2,000 Hz and different duty ratios in $NaAlO_2$ solution. The coatings are mainly composed of Al_2TiO_5. Increasing duty ratio, the congregation and the adsorption of Al from the electrolyte on the electrode surface is increased, and the redundant Al on the electrode results into the emergence of a little γ-Al_2O_3 in the coating. The change of the coating thickness is also related to the absorption layer of Al from the electrolyte and the solution speed of Ti under the fixed current density and frequency. Many residual discharging channels show that the spark discharge at 2,000 Hz is mainly attributable to the breakdown of the oxide film. And the coatings are formed both by the elements from the electrolyte and by the elements from the substrate; Al and Ti in the coating existed in the form of the reverse gradient distribution, meantime V from the substrate also came into the coatings in the form of amorphous state. Ceramic coatings improved corrosion resistance of Ti alloy and the coated samples prepared at $D = 20\%$ have the best corrosion resistance among the coated samples.

Acknowledgement This work was financially supported by Chinese Science Foundation for Post-doctor fellows (Grant No. 20060400238) and Harbin Special Foundation of Fellow Creation for Science and Technology of China (Grant No. 2006RFQXG032).

References

1. Yerokhin AL, Nie X, Leyland A, Matthews A, Dowey SJ (1999) Surf Coat Technol 122:73
2. Jiang BL, Zhang SF, Wu GJ, Lei TQ (2002) Chinese J Nonferrous Metals 12:454 (in Chinese)
3. Butygin PI, Khokhryakov YeV, Mamaev AL (2003) Mater Lett 57:1784
4. Tang ZL, Wang FH, Wu WT, Gordienko PS, Gnedenkov SV, Rudnev VS (1999) Chin J Nonferrous Metals 9:63 (in Chinese)
5. Liu YH, Li S (2006) Mater Protect 38:36 (in Chinese)
6. Pan JS, Li XL, Zhao WM (2005) Heat Treatment Metals 30:1 (in Chinese)
7. Атрощенко ЭС (1999) Известия ВУЗ чёрная металлургия 10:36 (in Russia)
8. Гнеденков СВ (2001) Защитаметаллов 37(2):192 (in Russia)
9. Yerokhin AL, Snizhko LO, Gurevina NL, Leyland A, Pilkington A, Matthews A (2004) Surf Coat Technol 177–178:779
10. Yerokhin AL, Leyland A, Matthews A (2002) Appl Surf Sci 200:172
11. Sundrarajan G, Rama Krishna L (2003) Surf Coat Technol 167:269
12. Verdier S, Boinet M, Maximovitch S, Dalard F (2005) Corros Sci 47:1429
13. Yang GL, Lv XY, Bai YZ, Cui HF, Jin ZS (2002) J Alloy Compd 345:196
14. Boguta DL, Rudnev VS, Gordienko PS (2004) Protect Metals 40:275
15. Yao ZP, Jiang ZH, Sun XT, Xin SG, Wu ZD (2005) Mater Chem Phys 92:408
16. Wang YM, Jiang BL, Lei TQ, Guo LX (2004) Mater Lett 58(12–13):1907
17. Xue WB, Wang C, Li YL, Deng ZW, Chen RY, Zhang TH (2002) Mater Lett 56:737
18. Yao ZP, Cui RH, Jiang ZH, Wang FP (2007) Appl Surf Sci 253:6778